# Lower Bounds to the *Q* Factor of Electrically Small Resonators Through Quasistatic Modal Expansion

Mariano Pascale<sup>®</sup>, Sander A. Mann<sup>®</sup>, Dimitrios C. Tzarouchis<sup>®</sup>, *Member, IEEE*, Giovanni Miano<sup>®</sup>, Andrea Alù<sup>®</sup>, *Fellow, IEEE*, and Carlo Forestiere<sup>®</sup>

Abstract—The problem of finding the optimal current distribution supported by small radiators yielding the minimum quality (Q) factor is a fundamental problem in electromagnetism. Q factor bounds constrain the maximum operational bandwidth of devices including antennas, metamaterials, and nanoresonators and have been featured in seminal papers in the past decades. Here, we determine the lower bounds of Q factors of small-size plasmonic and high-permittivity dielectric resonators, which are characterized by quasi-electrostatic and quasi-magnetostatic natural modes, respectively. We expand the induced current density field in the resonator in terms of these modes, leading to closed-form analytical expressions for the electric and magnetic polarizability tensors, whose largest eigenvalue is directly linked to the minimum Q factor. Our results also allow to determine in closed form the corresponding optimal current density field. In particular, when the resonator exhibits two orthogonal reflection symmetries, the minimum Q factor can be simply obtained from the Q factors of the single current modes with nonvanishing dipole moments aligned along the major axis of the resonator. Overall, our results open exciting opportunities in the context of nano-optics and metamaterials, facilitating the analysis and design of optimally shaped resonators for enhanced and tailored light-matter interactions.

Index Terms—Dielectric resonators, eigenvalues and eigenfunctions, plasmons, Q factors, resonances, scattering.

## I. INTRODUCTION

HU's limit [1] determines the minimum radiation quality (Q) factor of electrically small antennas. This limit applies to both self-resonant and non-self-resonant antennas,

Manuscript received 12 April 2022; revised 11 January 2023; accepted 27 January 2023. Date of publication 28 February 2023; date of current version 5 May 2023. This work was supported in part by the AFOSR MURI Program, and in part by the Simons Foundation. (Corresponding author: Carlo Forestiere.)

Mariano Pascale is with the Department of Electrical Engineering and Information Technology, Università degli Studi di Napoli Federico II, 80125 Naples, Italy, also with the Photonics Initiative, Advanced Science Research Center, City University of New York, New York, NY 10031 USA, and also with the ICFO-Institut de Ciencies Fotoniques, Barcelona Institute of Science and Technology, 08860 Barcelona, Spain.

Sander A. Mann is with the Photonics Initiative, Advanced Science Research Center, City University of New York, New York, NY 10031 USA.

Dimitrios C. Tzarouchis is with the Department of Electrical and System Engineering, University of Pennsylvania, Philadelphia, PA 19104 USA.

Giovanni Miano and Carlo Forestiere are with the Department of Electrical Engineering and Information Technology, Università degli Studi di Napoli Federico II, 80125 Naples, Italy (e-mail: carlo.forestiere@unina.it).

Andrea Alù is with the Photonics Initiative, Advanced Science Research Center, City University of New York, New York, NY 10031 USA, and also with the Physics Program, Graduate Center, City University of New York, New York, NY 10016 USA.

Color versions of one or more figures in this article are available at https://doi.org/10.1109/TAP.2023.3248442.

Digital Object Identifier 10.1109/TAP.2023.3248442

provided that a convenient tuning network is used for the latter. The minimum Q factor is associated with an optimal current distribution supported by the antenna. The search for such lower bounds originated with the works of Chu [1], Wheeler [2], and Harrington [3], and several techniques have been proposed over the years by many contributors including Collin and Rothschild [4] and McLean [5]. Thal [6], by restricting the sources to only the electric surface currents producing nonzero fields within the volume of the antenna, arrived at stricter bounds than his predecessors. Then, in a series of contributions, starting in [7], Gustafsson et al. provided shape-dependent bounds on the radiator's minimum Q, linking it to the available volume in which the search of the optimal current is constrained. They also reduced the variational problem of finding the minimum Q of antennas to determine the largest eigenvalues of the polarizability tensor. In subsequent years, Gustafsson and coworkers refined these ideas [8], [9], [10] exploiting the expressions for the reactive stored energy derived by Vandenbosch [11] and [12], Geyi et al. [13], and Geyi [14], and they also included magnetic-type antennas. Efficient numerical determination of the optimal current density field by expanding it in terms of the characteristic modes was also recently demonstrated by Chalas et al. [15], Capek and Jelinek [16], Jelinek and Capek [17], and Capek et al. [18]. Capek et al. [19] also recently investigated the role of symmetry in the evaluation of fundamental bounds. Yaghjian [20] has recently proven that the Chu lower bound on Q can be overcome using highly dispersive material to tune the antenna.

In the literature (e.g., [10], [11], [12]), the antennas are divided into two categories, depending on the features of the current density field they support. Antennas of the electric type support currents with zero curl, that is, longitudinal current density fields, while antennas of the magnetic type support currents with zero divergence, that is, transverse current density fields. As we shall see, this distinction naturally applies also to plasmonic and high-permittivity resonators. Plasmonic resonances [21], [22] emerge in scatterers made of dispersive materials with a negative real part of the permittivity (metals). In the small-size limit, the plasmonic resonances can be described within the quasi-electrostatic approximation of Maxwell's equations [23], [24], [25]: they are supported by quasi-electrostatic current density modes, which are longitudinal vector fields. On the other hand, dielectric resonances [26], [27] emerge in scatterers made of materials with a high and positive real part of the permittivity. In the small-size limit, the dielectric resonances can be described

by the quasi-magnetostatic approximation of Maxwell's equations [28]: they are supported by quasi-magnetostatic current density modes, which are transverse vector fields. Quasi-electrostatic and quasi-magnetostatic modes are the natural modes of the small-size scatterers [29].

This article tackles the problem of the lower bound of the Q factor for small-size plasmonic and dielectric resonators with arbitrary shape, expanding the current density field induced in the resonator in terms of its quasi-electrostatic or quasimagnetostatic density resonant modes. This expansion leads to: 1) the analytical and closed-form expressions of the electric and magnetic polarizability tensors of the resonator, whose eigenvalues have been linked to the minimum Q [7], [8]; 2) the analytical expression of the minimum Q from the dipole moments of the quasistatic current modes of the resonator; and 3) the closed-form expression of the optimal current. In particular, the determination of the optimal current without the use of an optimization procedure or the numerical solution of integral equations is a considerable advantage over other expansions, such as those based on the characteristic modes [30] of the resonator. This work also unveils the connection between the resonator's minimum Q factor and the Q factor of its natural modes. In particular, we have also found that the minimum Q factor of a resonator with two orthogonal reflection symmetries can be obtained from the Q factors of the single current modes with nonvanishing dipole moments along the major axis through their parallel combination. Moreover, when a plasmonic resonator supports a spatially uniform quasi-electrostatic current mode, this mode is guaranteed to have the minimum Q factor. Due to duality, when a dielectric resonator supports a curl-type quasimagnetostatic current mode of the form  $\hat{\mathbf{r}} \times \mathbf{c}$  where  $\mathbf{c}$  is a constant vector and  $\hat{\mathbf{r}}$  is the radial direction, this mode exhibits the minimum Q factor.

The article is organized as follows: in Section II we summarize the definition and main properties of the quasi-electrostatic and quasi-magnetostatic current modes of a small-sized scatterer of arbitrary shape. Then, in Section III, we address the problem of finding the minimum Q and the corresponding optimal current distribution by expanding the current density field induced in the resonator through its quasistatic current modes. In Section IV, many examples are shown, exemplifying the application of the introduced method to small-sized plasmonic and high-permittivity dielectric resonators of arbitrary shape. In Appendix A, we derive the expression of the Q factor for plasmonic and dielectric resonators from their stored energy and radiated power.

# II. RESONANCES OF SMALL-SIZE SCATTERERS

We consider a linear, homogeneous, isotropic, and nonmagnetic scatterer, occupying a volume V with boundary  $S = \partial V$  surrounded by vacuum. We define the characteristic linear dimension  $\ell_c$  of the scatterer to be the radius of the smallest sphere that surrounds it (see Fig. 1). We indicate with  $\chi(\omega)$  the susceptibility of the scatterer in the frequency domain, which we generally assume to be frequency dispersive. If  $\ell_c$  is much smaller than the operating wavelength, resonant electromagnetic scattering can occur due to different mech-

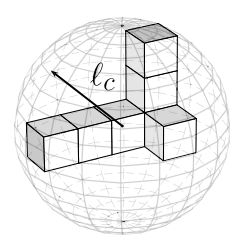


Fig. 1. Arbitrarily shaped plasmonic/dielectric resonator enclosed by the circumscribing "radiansphere" of radius  $\ell_c$ . In this work, we determine the lower bounds of Q factors of small- size plasmonic and dielectric resonators characterized by quasi-electrostatic and quasi-magnetostatic current modes.

anisms (e.g., [28], [31]), including plasmonic and dielectric resonances. In the following, we summarize the properties of the resonances and the resonant modes of solid scatterers. In Appendix B, we do the same for surface scatterers (i.e., shells).

## A. Plasmonic Resonances

Plasmonic resonances arise in small-size scatterers with a negative real part of the permittivity (e.g., metals). These resonances are associated with the eigenvalues of the integral operator that gives the electrostatic field as a function of the surface charge density on the surface S [23], [24]

$$\mathbf{j}_{h}^{\parallel}(\mathbf{r}) = \chi_{h}^{\parallel} \, \nabla_{\mathbf{r}} \oint_{S} \frac{\hat{\mathbf{n}}(\mathbf{r}') \cdot \mathbf{j}_{h}^{\parallel}(\mathbf{r}')}{4\pi \, |\mathbf{r} - \mathbf{r}'|} d^{2}\mathbf{r}' \quad \text{in } V.$$
 (1)

Here,  $\mathbf{j}_h^{\parallel}(\mathbf{r})$  is a quasi-electrostatic current mode of the scatterer and  $\chi_h^{\parallel}$  is the corresponding eigenvalue. The eigenvalues of this operator are discrete, real, positive, and size-independent, and  $\chi_h^{\parallel} \geq 2$  [24]. The quasi-electrostatic current modes are *longitudinal* vector fields in V: they are curl-free and div-free within V, but have a nonvanishing normal component on S [24]. These current modes are orthogonal, i.e.,

$$\left\langle \mathbf{j}_{h}^{\parallel}, \mathbf{j}_{k}^{\parallel} \right\rangle_{V} = \left\| \mathbf{j}_{h}^{\parallel} \right\|^{2} \delta_{h,k} \quad \forall h, k$$
 (2)

according to the scalar product

$$\langle \mathbf{f}, \mathbf{g} \rangle_V = \int_V \mathbf{f}^* \cdot \mathbf{g} \, d^3 \mathbf{r}.$$
 (3)

Moreover,  $\mathbf{j}_h^{\parallel}(\mathbf{r})$  satisfies the *charge-neutrality* condition  $\oint_S \sigma_h(\mathbf{r}) d^2\mathbf{r} = 0$ , where  $\sigma_h(\mathbf{r}) = (i\omega)^{-1} \mathbf{j}_h^{\parallel}(\mathbf{r}) \cdot \hat{\mathbf{n}}(\mathbf{r})$  is the surface charge density on S associated with the mode. The electric dipole moment of  $\mathbf{j}_h^{\parallel}(\mathbf{r})$  is

$$\mathbf{P}_{h} = \oint_{S} \sigma_{n}(\mathbf{r}) \mathbf{r} d^{2} \mathbf{r} = \frac{1}{i\omega} \int_{V} \mathbf{j}_{h}^{\parallel}(\mathbf{r}) d^{3} \mathbf{r}.$$
 (4)

If the mode  $\mathbf{j}_h^{\parallel}$  has a vanishing electric dipole moment, it is classified as *dark*, *bright* otherwise [32]. If the shape of the resonator has two orthogonal reflection symmetries, the dipole moment of each mode is aligned along one of these directions. When the scatterer has a quasi-electrostatic current mode  $\mathbf{j}_h^{\parallel} = \mathbf{c}$ , that is spatially uniform in V with direction  $\mathbf{c}$  (as it happens, for instance, in spheres and ellipsoids), the orthogonality condition (2) implies that all the remaining

current modes, i.e.,  $\mathbf{j}_k^{\parallel} \ \forall k \neq h$ , have a vanishing electric dipole moment along  $\mathbf{c}$ 

$$\mathbf{c} \cdot \int_{V} \mathbf{j}_{k}^{\parallel}(\mathbf{r}) d^{3}\mathbf{r} = (i\omega)\mathbf{c} \cdot \mathbf{P}_{k} = 0 \quad \forall k \neq h.$$
 (5)

The current density field J(r) induced in the scatterer by an incident electric field  $E_{inc}$  is given by [24], [31]

$$\mathbf{J}(\mathbf{r}) \approx i\omega\varepsilon_0 \sum_{h} \frac{\chi_h^{\parallel} \chi(\omega)}{\chi_h^{\parallel} + \chi(\omega)} \langle \mathbf{j}_h^{\parallel}, \mathbf{E}_{inc} \rangle_V \frac{\mathbf{j}_h^{\parallel}(\mathbf{r})}{\|\mathbf{j}_h^{\parallel}\|^2}$$
(6)

where  $\varepsilon_0$  is the vacuum permittivity. The resonance frequency  $\omega_h$  of the quasi-electrostatic current mode  $\mathbf{j}_h^{\parallel}$  is the frequency at which the real part of the denominator of (6) vanishes, i.e., [24]

$$\operatorname{Re}\{\chi(\omega_h)\} = -\chi_h^{\parallel}.\tag{7}$$

We now introduce the resonance size parameter  $\xi_h$ , defined as

$$\xi_h = \frac{\omega_h}{c_0} \ell_c \tag{8}$$

where  $c_0$  denotes the light velocity in vacuum. Assuming that the hth current mode  $\mathbf{j}_h^{\parallel}$  is bright and "isolated" (namely, its resonance frequency is sufficiently far from the resonance frequencies of the other modes), and the dispersion relation of the scatterer is of Drude type, we show in Appendix A1 that its Q factor has the following expression:

$$Q_h^{\parallel} = -3\ell_c^3 \frac{\oint_S \sigma_h^*(\mathbf{r}) \cdot \oint_S \frac{\sigma_h(\mathbf{r}')}{|\mathbf{r} - \mathbf{r}'|} d^2 \mathbf{r} d^2 \mathbf{r}'}{\oint_S \sigma_h^*(\mathbf{r}) \oint_S \sigma_h(\mathbf{r}') |\mathbf{r} - \mathbf{r}'|^2 d^2 \mathbf{r} d^2 \mathbf{r}'} \frac{1}{\xi_h^3}$$
(9)

which can also be rewritten as

$$Q_{h} = \frac{1}{\chi_{h}^{\parallel}} \frac{6\pi \|\mathbf{j}_{h}^{\parallel}\|^{2}}{\omega_{h}^{2} \|\mathbf{P}_{h}\|^{2}} \frac{\ell_{c}^{3}}{\xi_{h}^{3}} = \frac{1}{\chi_{h}^{\parallel}} \frac{6\pi \|\mathbf{j}_{h}^{\parallel}\|^{2}}{\|\int_{V} \mathbf{j}_{h}(\mathbf{r}) d^{3} \mathbf{r}\|^{2}} \frac{\ell_{c}^{3}}{\xi_{h}^{3}}.$$
 (10)

If the mode is dark, the Q factor presents a more complicated expression which diverges faster than  $1/\xi_h^3$  [31].

1) Modal Expansion of the Electric Polarizability Tensor: Following [33], the electric polarizability tensor of the scatterer is the linear correspondence,  $\overrightarrow{\gamma}_e$ :  $(E_0\hat{\mathbf{e}}) \rightarrow \mathbf{P}$ , between the electric field  $(E_0\hat{\mathbf{e}})$  and the electric dipole moment [34], [35]:

$$\mathbf{P} = \oint_{S} \sigma(\mathbf{r}) \mathbf{r} \, d^{2} \mathbf{r} \tag{11}$$

where  $\sigma(\mathbf{r})$  is the solution of the surface integral equation

$$\oint_{S} \frac{\sigma(\mathbf{r}')}{4\pi |\mathbf{r} - \mathbf{r}'|} d^{2}\mathbf{r}' = (\varepsilon_{0} E_{0} \hat{\mathbf{e}}) \cdot \mathbf{r} \quad \text{on } S$$
(12)

subjected to the charge neutrality condition;  $E_0$  is a real number and  $\hat{\mathbf{e}}$  is a unit vector.

We solve (12) by expanding the unknown  $\sigma$  in terms of the surface charge density modes  $\sigma_h$ , i.e.,  $\sigma(\mathbf{r}) = \sum_h \alpha_h \sigma_h(\mathbf{r})$ , on S. Substituting this expression in (12), which naturally satisfies the charge neutrality condition, multiplying both members by  $\sigma_k$ , integrating over the surface S, and exploiting the orthogonality condition (2), we obtain the

expression for the expansion coefficient  $\alpha_k$ . Thus, the dipole moment associated with the surface charge density  $\sigma$  is given by

$$\mathbf{P} = \sum_{h} \frac{\chi_{h}^{\parallel}}{\|\mathbf{j}_{h}^{\parallel}\|^{2}} \mathbf{P}_{h} \otimes \mathbf{P}_{h}(\varepsilon_{0} E_{0}) \hat{\boldsymbol{e}}$$
 (13)

where  $\otimes$  denotes the tensor product. From this, the electric polarizability tensor  $\overleftrightarrow{\gamma}_e$  is given by

$$\overleftrightarrow{\boldsymbol{\gamma}}_{e} = \sum_{h} \frac{\chi_{h}^{\parallel}}{\|\mathbf{j}_{h}^{\parallel}\|^{2}} \mathbf{P}_{h} \otimes \mathbf{P}_{h}. \tag{14}$$

This expression is the first important result of this work, as it relates in closed form the polarizability tensor to the quasi-electrostatic current modes of a plasmonic resonator.

#### B. Dielectric Resonances

Dielectric resonances arise in small-sized dielectric scatterers with large real part of permittivity. These resonances are associated with the eigenvalues of the magnetostatic integral operator that gives the vector potential as a function of the current density [28], [31]

$$\mathbf{j}_{h}^{\perp}(\mathbf{r}) = \frac{\chi_{h}^{\perp}}{\ell_{c}^{2}} \int_{V} \frac{\mathbf{j}_{h}^{\perp}(\mathbf{r}')}{4\pi |\mathbf{r} - \mathbf{r}'|} d^{3}\mathbf{r}' \quad \text{in } V$$
 (15)

with the condition  $\mathbf{j}_h^{\perp} \cdot \hat{\mathbf{n}}|_S = 0$ .  $\mathbf{j}_h^{\perp}(\mathbf{r})$  is a quasi-magnetostatic current mode of the scatterer, and  $\chi_h^{\perp}$  is the corresponding eigenvalue. The above equation holds in *weak* form in the functional space of the *transverse* vector fields equipped with the inner product (3). The spectrum of the magnetostatic integral operator (15) is discrete, and the eigenvalues are real and positive [28]. The quasi-magnetostatic current modes are transverse vector fields defined in V: they are div-free in V and have zero normal component on S. These modes are orthogonal, i.e.,

$$\langle \mathbf{j}_{h}^{\perp}, \mathbf{j}_{k}^{\perp} \rangle = \| \mathbf{j}_{h}^{\perp} \|^{2} \delta_{h,k} \quad \forall h, k.$$
 (16)

The electric dipole moments of the quasi-magnetostatic current modes are equal to zero. The magnetic dipole moment  $\mathbf{M}_h$  of the mode  $\mathbf{j}_h^{\perp}$  is

$$\mathbf{M}_{h} = \frac{1}{2} \int_{V} \mathbf{r} \times \mathbf{j}_{h}^{\perp}(\mathbf{r}) d^{3}\mathbf{r}. \tag{17}$$

If the shape of the scatterer has two orthogonal reflection symmetries, the magnetic dipole moment of each mode is aligned along either one of these directions. If the scatterer supports a mode of the form  $\mathbf{j}_h^{\perp} = \hat{\mathbf{r}} \times \mathbf{c}$ , where  $\mathbf{c}$  is a constant vector, then the orthogonality condition (16) implies that all the remaining modes  $\mathbf{j}_k^{\perp}$  with  $k \neq h$  have a vanishing magnetic dipole moment along  $\mathbf{c}$ 

$$\int_{\mathcal{U}} \mathbf{j}_k^{\perp} \cdot (\hat{\mathbf{r}} \times \mathbf{c}) d^3 \mathbf{r} = -2\mathbf{c} \cdot \mathbf{M}_k = 0, \quad k \neq h.$$
 (18)

For a small dielectric scatterer with high permittivity, the current density field  $\mathbf{J}(\mathbf{r})$  induced in V by an incident electric field  $\mathbf{E}_{inc}$  is [28]

$$\mathbf{J}(\mathbf{r}) \approx i\omega\varepsilon_0 \sum_{h} \frac{\chi(\omega)\chi_h^{\perp}}{\chi_h^{\perp} - \frac{\omega^2\ell_c^2}{c^2}\chi(\omega)} \langle \mathbf{j}_h^{\perp}, \mathbf{E}_{inc} \rangle_V \frac{\mathbf{j}_h^{\perp}(\mathbf{r})}{\|\mathbf{j}_h^{\perp}\|^2}. \quad (19)$$

The resonance frequency of the quasi-magnetostatic current mode  $\mathbf{j}_h^{\perp}$  is the frequency  $\omega_h$  at which the real part of the denominator of (19) vanishes

$$\operatorname{Re}\{\chi(\omega_h)\} = \frac{\omega_h^2 \ell_c^2}{c_0^2} \chi_h^{\perp}.$$
 (20)

In Appendix A2, we show that if the hth mode has a nonvanishing magnetic dipole moment, its Q factor is

$$Q_{h}^{\perp} = 6\pi \frac{\|\mathbf{j}_{h}^{\perp}\|^{2}}{\|\mathbf{M}_{h}^{\perp}\|^{2}} \frac{\ell_{c}^{5}}{\chi_{h}^{\perp}} \frac{1}{\xi_{h}^{3}}$$

$$= 6\ell_{c}^{3} \frac{\int_{V} \mathbf{j}_{h}^{\perp}(\mathbf{r}) \cdot \int_{V} \frac{\mathbf{j}_{h}^{\perp}(\mathbf{r}')}{|\mathbf{r} - \mathbf{r}'|} d^{3}\mathbf{r}' d^{3}\mathbf{r}}{\int_{V} \mathbf{j}_{h}^{\perp}(\mathbf{r}) \cdot \int_{V} \mathbf{j}_{h}^{\perp}(\mathbf{r}') |\mathbf{r} - \mathbf{r}'|^{2} d^{3}\mathbf{r}' d^{3}\mathbf{r}} \frac{1}{\xi_{h}^{3}}. \quad (21)$$

1) Modal Expansion of the Polarizability Tensor: Following [33], the magnetic polarizability tensor  $\overrightarrow{\gamma}_m$  is the linear correspondence,  $\overrightarrow{\gamma}_m: (H_0\hat{\mathbf{e}}) \to \mathbf{M}$ , between  $H_0\hat{\mathbf{e}}$  ( $H_0$  is a real number and  $\hat{\mathbf{e}}$  is a unit vector) and the magnetic dipole moment  $\mathbf{M}$  of the current density field  $\mathbf{j}$  with zero average over V that is the solution of the integral equation [10]:

$$\int_{V} \frac{\mathbf{j}(\mathbf{r}')}{4\pi |\mathbf{r} - \mathbf{r}'|} d^{3}\mathbf{r}' = \frac{1}{2} (H_{0}\hat{\mathbf{e}}) \times \mathbf{r}, \quad \text{in } V.$$
 (22)

To solve (22), we expand the current density **j** in terms of the quasi-magnetostatic current modes. As we have done in the solution of the integral equation (12), we obtain the expression for  $\overrightarrow{\gamma}_m$ 

$$\overleftrightarrow{\boldsymbol{\gamma}}_{m} = \sum_{h} \frac{\chi_{h}^{\perp}}{\|\mathbf{j}_{h}^{\perp}\|^{2}} \mathbf{M}_{h} \otimes \mathbf{M}_{h}. \tag{23}$$

As a second important result of this work, this relation expresses in closed form the polarizability tensor as a function of the quasi-magnetostatic current modes.

# III. MINIMUM Q FACTOR AND OPTIMAL CURRENT DISTRIBUTION FOR PLASMONIC/ DIELECTRIC RESONATORS

We now tackle the problem of determining the optimal current distribution that supports the minimum Q factor for small-sized plasmonic and high-permittivity dielectric resonators.

### A. Plasmonic Resonators

The problem of finding the minimum Q consists of determining the optimal current density  $\mathbf{j}$  in the functional space of longitudinal vector fields defined in V, which gives the minimum value of the functional

$$\xi^{3}Q = -3\ell_{c}^{3} \frac{\oint_{S} \sigma^{*}(\mathbf{r}) \cdot \oint_{S} \frac{\sigma(\mathbf{r}')}{|\mathbf{r} - \mathbf{r}'|} d^{2}\mathbf{r} d^{2}\mathbf{r}'}{\oint_{S} \sigma^{*}(\mathbf{r}) \oint_{S} \sigma(\mathbf{r}') |\mathbf{r} - \mathbf{r}'|^{2} d^{2}\mathbf{r} d^{2}\mathbf{r}'}$$
(24)

where  $\xi = \omega \ell_c / c_0$  and  $\mathbf{j} \cdot \mathbf{n} = \sigma / (i\omega)$ . This expression of the Q factor and the following derivation also hold for surface scatterers provided that the quantity  $\mathbf{j} \cdot \mathbf{n}$  is replaced by  $\nabla_s \cdot \mathbf{j}$ .

Vandenbosch [12] showed that the minimization of functional (24) can be successfully achieved by recasting minimization as the problem of finding the zeros of a matrix determinant. Here, we choose to follow the approach of Gustafsson et al. [7] and [8] and Jonsson and Gustafsson [10].

They found that any pair  $(\sigma_{opt}, \gamma)$  satisfying the integral equation [7], [8], [10]

$$\oint_{S} \frac{\sigma_{opt}(\mathbf{r}')}{4\pi |\mathbf{r} - \mathbf{r}'|} d^{2}\mathbf{r}' - \gamma \frac{1}{\ell_{c}^{3}} \mathbf{r} \cdot \oint_{S} \sigma_{opt}(\mathbf{r}') \mathbf{r}' d^{2}\mathbf{r}' = 0, \quad \text{on } S$$
(25)

gives a local minimum of the functional  $\xi^3 Q$  ( $\gamma$  is the Lagrange multiplier), and among them the absolute minimum can be found. In particular, they found that the minimum of the Q factor is given by [7], [10]

$$\left(\xi^3 Q\right)_{\min} = \frac{6\pi \ell_c^3}{\nu_{\text{e max}}} \tag{26}$$

where  $\gamma_{e,\text{max}}$  is the maximum among the three eigenvalues of the electric polarizability tensor  $\stackrel{\longleftarrow}{\gamma}_e$ . Equation (26) is also consistent with the formula found by Yaghjian and coworkers in [36] [see (44)]. The corresponding eigenvector returns the direction of the dipole moment  $\hat{\mathbf{p}}_{\text{opt}}$  of the optimal surface charge density  $\sigma_{opt}$ 

$$\hat{\mathbf{p}}_{\text{opt}} = \int_{S} \sigma_{opt}(\mathbf{r}) \mathbf{r} \, d^2 \mathbf{r}. \tag{27}$$

We now expand the optimal current distribution  $\mathbf{j}_{\text{opt}}$  in terms of the quasi-electrostatic current modes  $\mathbf{j}_h^{\parallel}$ ,  $\mathbf{j}_{\text{opt}}(\mathbf{r}) = \sum_h \alpha_h \mathbf{j}_h^{\parallel}(\mathbf{r})$ . We determine the coefficients  $\alpha_h$  by substituting this expansion in the critical equation (25), using (27) and the orthogonality (2). Eventually, we obtain

$$\mathbf{j}_{\text{opt}}(\mathbf{r}) = \sum_{h} \frac{\chi_{h}^{\parallel}}{\|\mathbf{j}_{h}^{\parallel}\|^{2}} (\hat{\mathbf{p}}_{\text{opt}} \cdot \mathbf{P}_{h}) \mathbf{j}_{h}^{\parallel}(\mathbf{r}). \tag{28}$$

This is a third remarkable result of this work: once the direction of the dipole moment associated with the optimal current is determined, the optimal current is known in closed form. This property constitutes a significant advantage over the previously developed techniques for electrically small antennas, as in [7], [8], and [12], for which the determination of the optimal current is not straightforward because it requires the solution of an integral equation. As we shall see in Section IV, only a few quasi-electrostatic modes are needed to achieve a good estimate of the optimal current.

If the shape of the resonator has two orthogonal reflection symmetry planes with normals  $\hat{\mathbf{e}}_1$  and  $\hat{\mathbf{e}}_2$ , the principal axes of  $\overrightarrow{\gamma}_e$  are the triplet  $(\hat{\mathbf{e}}_1, \hat{\mathbf{e}}_2, \hat{\mathbf{e}}_3)$ , where  $\hat{\mathbf{e}}_3$  is orthogonal to both  $\hat{\mathbf{e}}_1$  and  $\hat{\mathbf{e}}_2$ . The dipole moments of the quasi-electrostatic current modes are also aligned along these directions. In this case, the three occurrences of  $\overrightarrow{\gamma}_e$  are obtained from (14). They are given by

$$\gamma_{e,i} = \sum_{h} \frac{\chi_h^{\parallel}}{\|\mathbf{j}_h^{\parallel}\|^2} \left| \hat{\mathbf{e}}_i \cdot \mathbf{P}_h \right|^2, \quad i = 1, 2, 3.$$
 (29)

Only the quasi-electrostatic current modes with dipole moment directed along  $\hat{\mathbf{e}}_i$  contribute to the sum. In this

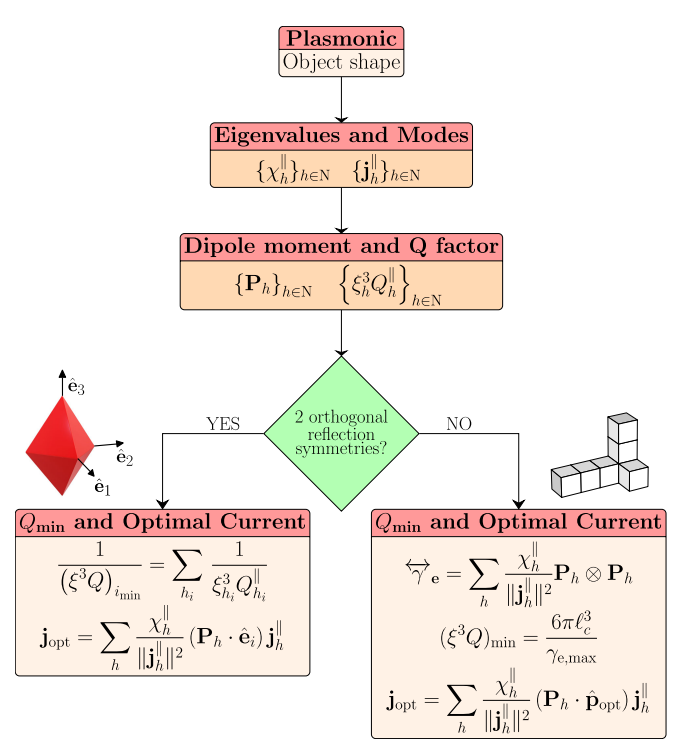


Fig. 2. Flowchart for the calculation of the minimum Q factor of an arbitrarily shaped plasmonic resonator using the quasi-electrostatic current modes. First, we preliminarily calculate the current modes. Then, if the scatterer has two reflection symmetries, the minimum Q along the principal axis of the electric polarizability tensor  $\hat{\bf e}_1$ ,  $\hat{\bf e}_2$ , and  $\hat{\bf e}_3$  is obtained from the Q factor of the current modes with nonvanishing dipole moments oriented along that axis. The absolute minimum Q is the minimum value among these tree values, which corresponds to the optimal current. If no such symmetries are present, then we analytically assembly the polarizability tensor using the dipole moments and the eigenvalues of the modes, and eventually we find its eigenvalues and eigenvectors. The minimum Q and optimal currents are then immediately obtained. A similar flowchart can be drawn for a high-permittivity dielectric resonator

case, by combining (29), (26), and (10), we obtain a fourth important result of this work: the minimum Q along the axis  $\hat{\mathbf{e}}_i$  is given by the parallel formula

$$\frac{1}{(\xi^3 Q)_{\min,i}} = \sum_{h_i} \frac{1}{\xi_{h_i}^3 Q_{h_i}^{\parallel}}$$
 (30)

where the label  $h_i$  denotes the modes with nonvanishing electric dipole moments along  $\hat{\mathbf{e}}_i$ . As shown in (5), due to the modes' orthogonality, if there exists a current mode spatially uniform along  $\hat{\mathbf{e}}_i$ , it is also the only current mode with nonvanishing dipole moment along  $\hat{\mathbf{e}}_i$ , and then it necessarily exhibits the minimum Q factor.

In conclusion, we summarize in Fig. 2 the algorithm to determine the minimum Q factor and the corresponding optimal current of an arbitrary shaped plasmonic resonator.

## B. High-Permittivity Dielectric Resonators

The problem of finding the minimum Q consists in determining the optimal current density  $\mathbf{j}$ , in the functional space of transverse vector fields defined in V, which gives the minimum value of the functional

$$\xi^{3}Q = 6\ell_{c}^{3} \frac{\int_{V} \mathbf{j}(\mathbf{r}) \cdot \int_{V} \frac{\mathbf{j}(\mathbf{r}')}{|\mathbf{r} - \mathbf{r}'|} d^{3}\mathbf{r} d^{3}\mathbf{r}'}{\int_{V} \mathbf{j}(\mathbf{r}) \cdot \int_{V} \mathbf{j}(\mathbf{r}') |\mathbf{r} - \mathbf{r}'|^{2} d^{3}\mathbf{r} d^{3}\mathbf{r}'}$$
(31)

where  $\mathbf{j}$  is the current density field. The above expression also holds for surface scatterers of high-conductivity, provided that the volume integrals are replaced by surface integrals.

The minimum Q factor is obtained from the maximum eigenvalue  $\gamma_{m,\text{max}}$  of the magnetic polarizability tensor  $\overrightarrow{\gamma}_m$  [10]

$$\left(\xi^3 Q\right)_{\min} = \frac{6\pi \ell_c^3}{\nu_{m,\max}}.$$
 (32)

Since the magnetic polarizability tensor has the closed-form expression (23), the determination of  $(\xi^3 Q)_{\min}$  only requires the calculation of the eigenvalues of a 3 × 3 matrix. Equation (32) is also consistent with the formula found by Yaghjian and coworkers in [36]. The eigenvector corresponding to  $\gamma_{m,\max}$  returns the direction  $\hat{\mathbf{m}}_{\text{opt}}$  of the dipole moment of the optimal current. Following the same steps we have done for the plasmonic resonator, the optimal current is readily obtained in terms of the quasi-magnetostatic current modes:

$$\mathbf{j}_{\text{opt}}(\mathbf{r}) = \sum_{h} \chi_{h}^{\perp} (\hat{\mathbf{m}}_{\text{opt}} \cdot \mathbf{M}_{h}) \mathbf{j}_{h}^{\perp}(\mathbf{r}). \tag{33}$$

As we will see in Section IV, in many scenarios, only a few current modes have to be considered to have a good estimation of the minimum Q factor.

As for the plasmonic resonators, if the shape of the resonator has two orthogonal reflection symmetry planes with normals  $\hat{\mathbf{e}}_1$  and  $\hat{\mathbf{e}}_2$ , the principal axis of  $\overrightarrow{\boldsymbol{\gamma}}_m$  is the triplet  $(\hat{\mathbf{e}}_1, \hat{\mathbf{e}}_2, \hat{\mathbf{e}}_3)$ , where  $\hat{\mathbf{e}}_3$  is orthogonal to both  $\hat{\mathbf{e}}_1$  and  $\hat{\mathbf{e}}_2$ . Thus, the three occurrences of  $\overrightarrow{\boldsymbol{\gamma}}_m$  are

$$\gamma_{m,i} = \sum_{h} \frac{\chi_h^{\perp}}{\|\mathbf{j}_h^{\perp}\|^2} \left| \hat{\mathbf{e}}_i \cdot \mathbf{M}_h \right|^2, \quad i = 1, 2, 3$$
 (34)

where the summation runs only over the quasi-magnetostatic current modes with magnetic dipole moment directed along  $\hat{\mathbf{e}}_i$ . The minimum Q along the axis  $\hat{\mathbf{e}}_i$  is then obtained by their parallel combination

$$\frac{1}{(\xi^3 Q)_{\min,i}} = \sum_{h_i} \frac{1}{\xi_{h_i}^3 Q_{h_i}^{\perp}}$$
 (35)

where only the modes with magnetic dipole moment directed along  $\hat{\mathbf{e}}_i$  have to be considered. In addition, as shown in (18), due to the modes' orthogonality, if there exists a current curl-type mode in the form  $\mathbf{r} \times \mathbf{c}$ , it is the only one with nonvanishing magnetic dipole moment along direction  $\mathbf{c}$ . Thus, it necessarily has the minimum Q factor.

# IV. RESULTS AND DISCUSSION

We now exemplify the outlined method, by evaluating the minimum Q factor of small-sized plasmonic and dielectric resonators with different shapes. We first consider shapes that support uniform quasi-electrostatic modes and curl-type quasi-magnetostatic modes, which are guaranteed to have the minimum Q factor. Then, we consider shapes with two orthogonal reflection symmetries, where the minimum Q factor can be obtained from the Q factors of the quasi-static current modes through the parallel formula. Eventually, we consider shapes with no symmetry. The electrostatic eigenvalue problem (1) is solved by the numerical method outlined in [23] and [37],

and the magnetostatic eigenvalue problem (15) is solved by the numerical method described in [28] and [38].

#### A. Plasmonic Resonator

1) Shapes With Uniform Current Modes: A sphere with unit radius has three degenerate quasi-electrostatic uniform current modes, one for each of the three orthogonal direction  $\hat{\mathbf{x}}$ ,  $\hat{\mathbf{y}}$ ,  $\hat{\mathbf{z}}$ , with eigenvalues  $\chi_{x,y,z}^{\parallel} = 3$ . We show the surface charge density of the current mode  $\mathbf{j}_z^{\parallel} = \sqrt{3/(4\pi)}\,\hat{\mathbf{z}}$  in Fig. 3(a). For the considerations made in Section III-A, these modes are the *only* bright modes supported by a sphere. Thus, their Q factors coincide with the minimum Q factor supported by the sphere for longitudinal currents

$$(\xi^3 Q)_{\min} = \xi_{x,y,z}^3 Q_{x,y,z}^{\parallel} = 1.5.$$
 (36)

Similarly, a rotationally symmetric spheroid (around  $\hat{\mathbf{z}}$ ) has three uniform current modes,  $\mathbf{j}_x^{\parallel} = j_0 \hat{\mathbf{x}}$ ,  $\mathbf{j}_y^{\parallel} = j_0 \hat{\mathbf{y}}$ , and  $\mathbf{j}_z^{\parallel} = j_0 \hat{\mathbf{z}}$ , where  $j_0 = 1/\sqrt{V}$  and  $V = (4/3)\pi a_x^2 a_z$ , where  $a_x$  and  $a_z$  are the semi-axis. They are the *only* bright modes of the spheroid. The expression (10) for the Q factor in this case simplifies to

$$\xi_{x,y,z}^{3} Q_{x,y,z}^{\parallel} = \frac{6\pi \ell_c^3}{V} \frac{1}{\chi_{x,y,z}^{\parallel}}.$$
 (37)

The eigenvalue  $\chi_h^{\parallel}$  corresponding to the current mode aligned along the major axis is the maximum eigenvalue, and therefore, the minimum Q is associated with it. As an example, in Fig. 3(a), we consider the case of a prolate and an oblate spheroid with aspect ratio 2:1.

2) Shapes With Nonuniform Current Modes and Two Reflection Symmetries: We consider a rod with radius R and height H = 4R, aligned along  $\hat{\mathbf{z}}$ . We modeled the rod as a superellipsoid, with boundary  $(x/R)^2 + (y/R)^2 + (z/(4R))^{10} = 1$ . We follow the algorithm outlined in Fig. 2. In Fig. 3(b), on the right of the "=" sign, we show the surface charge density of the three bright modes with lowest Q and with electric dipole moment directed along  $\hat{z}$ . We obtain the minimum Q factor by combining the Q factor of the bright modes using the parallel formula and the optimal current by applying (28). In the same figure, on the left of the "=" sign we show the charge density corresponding to the minimum Q factor. The Q factor of the first current mode is very close to the Q bound because for the considered superellipsoid, the first current mode on the right of the equal sign is almost uniform. The relative error in the calculation of  $(\xi^3 Q)_{\min}$  by considering only the first three current modes is below 0.2%.

In Fig. 3(c), we also consider the case of a sphere dimer of radius R, aligned along the  $\hat{\mathbf{z}}$ -axis with an edge–edge gap  $\delta = R/10$ . Similar to the rod, the minimum Q factor is obtained by combining the Q factor of the bright modes with electric dipole moments aligned along the  $\hat{\mathbf{z}}$ -axis, using the parallel formula. On the other hand, for the sphere dimer the first mode exhibits a Q that is quite larger than the minimum. This is because the dimer of two nearly touching spheres supports modes that strongly deviate from the uniform distribution [39]. The relative error in the calculation of  $(\xi^3 Q)_{\min}$  by considering only the first three modes is below 0.3%.

3) Shapes With Nonuniform Current Modes and No Symmetries: We consider a block with three arms of different lengths. We first compute the quasi-electrostatic modes of this scatterer. The four bright modes with lowest Q factor are shown in Fig. 3 on the right of the "=" sign. The direction of the dipole moment  $\mathbf{P}_h$  of each mode is also shown in the insets. Considering that there are no symmetries, we have to preliminary assemble the polarizability tensor using (12) and find its maximum eigenvalue. On the left of Fig. 3(d), we show the surface charge density associated with the optimal current obtained by (28). The relative error in the estimation of  $(\xi^3 Q)_{\min}$  by taking into account only the four modes shown in Fig. 3(d) is 26%. We have to consider at least 25 modes to have an error below 10%.

#### B. Dielectric Resonator

1) Shapes Supporting a Quasi-Magnetostatic Curl-Type Mode: We now consider a dielectric resonator having the shape of a spherical shell with unit radius. First, we compute the quasi-magnetostatic current modes associated with this shape by (65) of Appendix B2. This shape supports three degenerate current curl-type modes with nonzero magnetic dipole moment:  $\mathbf{j}_{\hat{\mathbf{c}}}^{\perp} = \sqrt{3/(2\pi)}\,\hat{\mathbf{r}}\,\times\hat{\mathbf{c}}$  where  $\hat{\mathbf{c}} = \hat{\mathbf{x}},\hat{\mathbf{y}},\hat{\mathbf{z}}$ ; the magnetic dipole moment is oriented along  $\hat{\mathbf{c}}$  and  $\chi_{\hat{\mathbf{c}}}^{\perp} = 3$ . According to the discussion of Section II-B, they are the only modes with nonvanishing magnetic dipole moment. We show one of these current modes in Fig. 3(e). Thus, applying (35) the minimum Q factor is

$$(\xi^3 Q)_{\min} = (\xi_{\hat{\mathbf{r}}}^3 Q_{\hat{\mathbf{r}}}^{\perp}) = 3.$$
 (38)

This is in agreement with [6], [9], and [12].

2) Shapes With Two Reflection Symmetries: We now consider a dielectric sphere resonator of unit radius. Unlike the spherical shell, the solid sphere does not support a mode of the form  $\hat{\bf r} \times {\bf c}$ . We compute the supported quasi-magnetostatic current modes solving the eigenvalue problem (15). We limit our analysis to the ones having nonvanishing magnetic dipole moment along the  $\hat{\bf z}$ -axis:  ${\bf j} \frac{1}{h}(r,\theta,\phi) = \sqrt{3\pi}/2 \ j_1(h\pi r) \ \hat{\bf r} \times \hat{\bf z}$ , where  $h \in \mathbb{N}$  and  $j_1$  is the spherical Bessel function of the first kind and order 1. They are associated with the eigenvalues  $\chi_h^\perp = (h\pi)^2$ . The Q factors of the modes are  $(\xi_h^3 Q_h^\perp) = (h\pi)^2/2$ . The first three current modes are shown on the right of the "=" sign in Fig. 3(f), with their Q factor. The minimum Q factor  $(\xi^3 Q)_{\min}$  is obtained by applying (35)

$$(\xi^3 Q)_{\min}^{-1} = \sum_{h} (\xi_h Q_h^{\perp})^{-1} = \frac{2}{\pi^2} \sum_{h} \frac{1}{h^2} = \frac{2}{\pi^2} \frac{\pi^2}{6} = \frac{1}{3}$$
 (39)

which is in agreement with Thal's analysis. In this parallel, by only considering the first four modes, we obtain an error of 15.4%; we have to consider at least 13 modes to have an error below 5%. The current density field is obtained by applying (33)

$$\mathbf{j}_{opt}(r,\theta,\phi) = \sqrt{\frac{3}{2\pi}} \,\delta(r-1)\,\hat{\mathbf{r}} \times \hat{\mathbf{z}} \tag{40}$$

where  $\delta$  is a Dirac delta function. Thus, it corresponds to a surface current localized on the sphere's surface, which is the same optimal current found for a spherical shell.

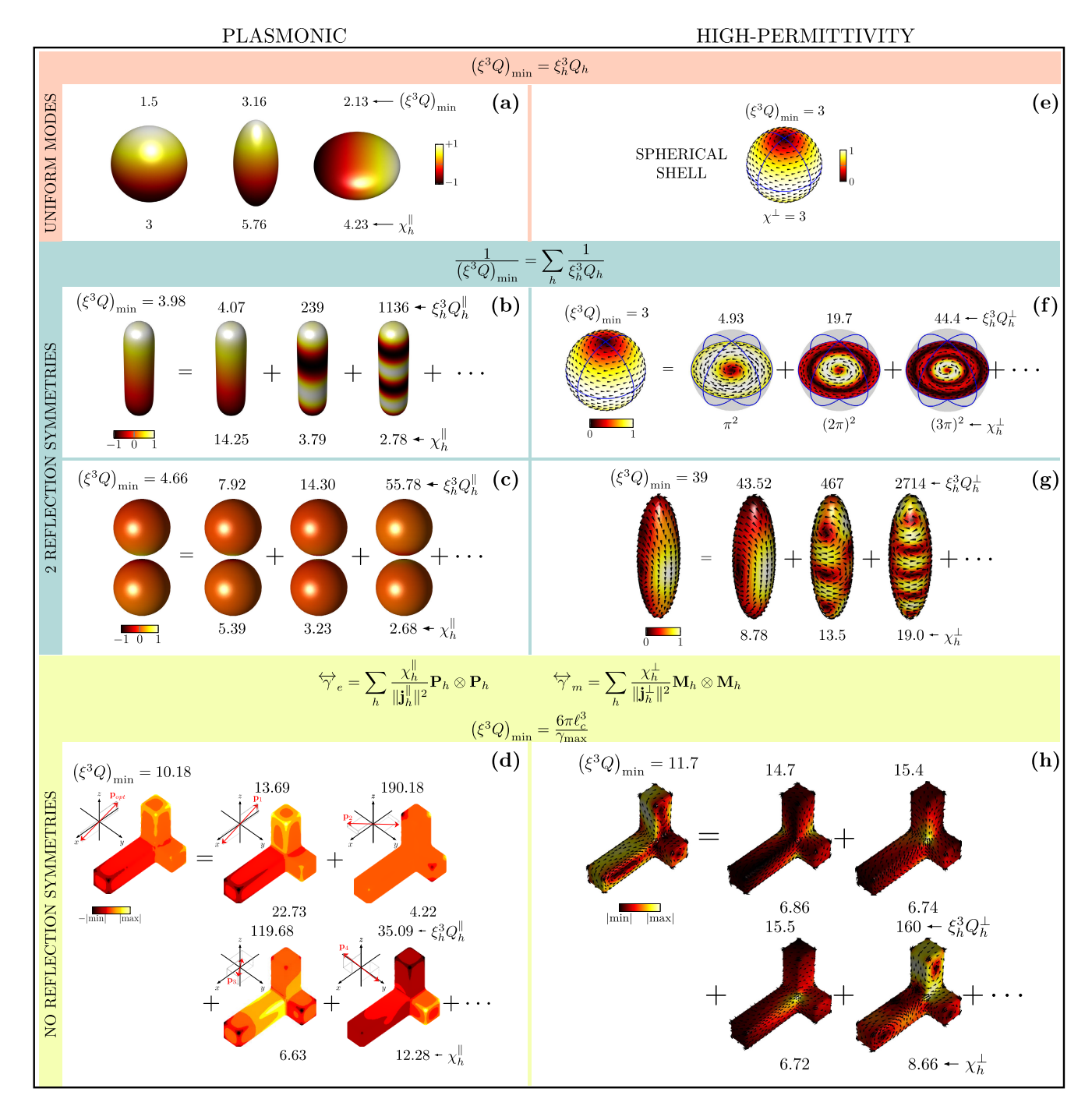


Fig. 3. Minimum Q and corresponding optimal charge/current distribution supported by (a)–(d) plasmonic and (e)–(h) dielectric resonators. Plasmonic resonators. (a) Optimal charge density supported by a sphere and by prolate and oblate spheroids with aspect ratio 2:1; the bright modes of these shapes are the uniform current modes. Optimal charge density supported by geometries exhibiting two reflection symmetries, namely, (b) rod and (c) sphere's dimer, and (d) by a shape without symmetries. In (b)–(d), on the right of the "=" sign, plasmonic modes with lowest Q factor, their Q factor (top), and eigenvalues (bottom). The colormap represents the electric charge density. Dielectric resonators. (e) Current density mode of a spherical shell of the form  $\hat{\mathbf{r}} \times \mathbf{c}$  that is the optimal current density for the spherical shell. Optimal current density supported by geometries exhibiting two reflection symmetries, namely, (f) solid sphere and (g) ellipsoid, and (h) by a shape with no symmetries. In each panel, on the right of the "=" sign, quasi-magnetostatic modes with lowest Q factor, their individual Q factor (top), and eigenvalues (bottom). The colormap represents the magnitude of the current density, the arrows its direction.

We now consider a spheroidal shell with aspect ratio 4:1, with major axis aligned along  $\hat{\mathbf{z}}$ . Also this shape does not support a curl-type mode. We compute the quasi-magnetostatic resonances by solving the eigenvalue problem (65) of Appendix B2. The minimum Q factor is associated with the set of quasi-magnetostatic modes exhibiting a nonvanishing

magnetic dipole moment along the major axis. In Fig. 3(g), we show the optimal surface current, the eigenvalues, and Q factor of the three current modes with the lowest Q factor. The value of the minimum Q factor is obtained using (35):  $(\xi^3 Q)_{\min} = 39$ . If we only consider the three modes shown in Fig. 3(g), an error < 1% is obtained.

3) Shapes With No Symmetries: We consider a shell with no reflection symmetries, defined as the boundary of a block with three arms of different lengths. We preliminarily compute its quasi-magnetostatic current modes by solving (65), their magnetic dipole moments  $\mathbf{M}_h$  by (17), and Q factors by (21). The four modes with the lowest Q factor are shown in Fig. 3(h) on the right of the equality sign, with their Q factor (above) and eigenvalue (below). We assembly the magnetic polarizability tensor  $\overrightarrow{\gamma}_m$  using (23) from the dipole moments of the current modes  $\mathbf{M}_h$ . The maximum eigenvalue  $\gamma_{max}$  of  $\overrightarrow{\gamma}_m$  gives the minimum Q factor through (26). The optimal current obtained using (33) is shown on the left of the equality sign in Fig. 3(h). Only by considering the first three modes, we obtain an estimate of  $(\xi^3 Q)_{min}$  with an error of 12%.

#### V. Conclusion

We have tackled the problem of finding the minimum Q and the optimal current of electrically small plasmonic and high-index nano-resonators, a topic of great relevance for the growing metamaterials and nano-optics community. We show that this electromagnetic problem is conveniently described in a basis formed by the quasistatic resonance modes supported by the scatterer, which are the natural modes of the resonator in the small-size limit. We demonstrated that the expansion of the current density in terms of quasistatic modes leads to analytical closed-form expressions for the electric and magnetic polarizability tensors, whose eigenvalues are directly linked to the minimum Q. Hence, we have been able to determine the minimum Q and the corresponding optimal current distributions in the scatterers in closed form. In particular, we found that when the resonator exhibits two orthogonal reflection symmetries, its minimum Q factor can be simply obtained from the Q factors of the quasistatic modes of the radiator with nonvanishing dipole moment along with the major axis. Moreover, when a plasmonic resonator supports a spatially uniform quasi-electrostatic current mode, this mode is guaranteed to have the minimum Q factor. Because of duality, when a dielectric resonator supports a quasi-magnetostatic current, curl-type mode, in form  $\hat{\mathbf{r}} \times \mathbf{c}$  where  $\mathbf{c}$  is a constant vector and  $\hat{\mathbf{r}}$  is the radial direction, this mode also exhibits the minimum Q factor. The introduced method can also be applied to find the minimum Q of translational invariant scatterers [40].

In this article, we considered plasmonic and highpermittivity resonant scatterers, limiting the search space for optimal currents either to longitudinal or transverse current density vector fields [16]. However, in principle, lower bounds may be obtained by simultaneously considering both types of vector fields [16], e.g., in dual-mode antennas [9].

Beyond the limit of small-size resonators, the advantages of the quasistatic basis become less relevant, and the use of convex optimization over current density becomes necessary [15], [16], [17], [18] to find the minimum Q. Nevertheless, since the quasi-electrostatic and quasi-magnetostatic modes form a basis for the square-integrable currents defined within the scatterer, they can be used to represent the optimal current solution of convex optimization problems. We expect that the optimal

current in the Drude plasmonic particle will no longer be irrotational (as in the small-particle limit). Dually, the optimal current in high-index resonator will no longer be solenoidal. In both the cases, the contribution of both the electrostatic and magnetostatic modes will be needed to determine the optimal current; nevertheless, if the size of the scatterer is smaller or comparable to the resonance frequency, we expect that only few modes will be required to describe the optimal current.

The introduced framework bridges a classic antenna problem to the field of resonant scattering, and in particular to the field of plasmonics, metamaterials, and nano-optics. Our results may be especially appealing to researchers and engineers working in photonics and polaritonics, leading to optimal solutions to enable enhanced light-matter interactions through engineered nanostructures.

#### APPENDIX

# A. Q Factor of Small Scatterers

In this Appendix, we derive the expression of the Q factor for plasmonic and high-permittivity resonators with characteristic dimension  $\ell_c$  much smaller than the operating wavelength  $\lambda$ ,  $\xi = 2\pi \ell_c/\lambda \ll 1$ . The Q factor of a self-resonant structure is defined as  $2\pi$  times the ratio between the mean value over the cycle of the stored energy  $\mathscr{W}_{\text{stored}}$  and the energy  $\mathscr{W}_{\text{lost}}$  lost per cycle by damping processes, both evaluated at the resonance frequency of the h-th mode  $\omega_h$  (e.g., [41], [42])

$$Q \stackrel{\text{def}}{=} 2\pi \times \frac{\mathscr{W}_{\text{stored}}}{\mathscr{W}_{\text{lost}}} = \omega_h \times \frac{\mathscr{W}_{\text{stored}}}{\text{power loss}}.$$
 (41)

1) Plasmonic Resonator: In this section, we evaluate the stored energy, the radiated power, and the Q factor of a dispersive plasmonic scatterer. We describe the metal using the Drude model (e.g., [21]) with vanishing dissipation losses

$$\chi(\omega) = -\frac{\omega_p^2}{\omega(\omega + i\nu)} \approx -\frac{\omega_p^2}{\omega^2}$$
 (42)

where  $\omega_p$  is the plasma frequency and  $\nu$  is the damping rate of the free electrons of the metal, which is assumed to be much smaller than  $\omega_p$  and the operating frequency  $\omega$ .

a) Mean value of the stored energy: The electrostatic field  $\mathbf{E}_h$  associated with the surface charge density  $\sigma_h$  of the quasi-electrostatic (plasmon) current mode  $\mathbf{j}_h^{\parallel}$  is given by [24]

$$\mathbf{E}_{h}(\mathbf{r}) = -\frac{\nabla_{\mathbf{r}}}{4\pi\,\varepsilon_{0}} \oint_{S} \frac{\sigma_{h}(\mathbf{r}')}{|\mathbf{r} - \mathbf{r}'|} dS'. \tag{43}$$

The mean value of the energy stored in the whole space  $\mathcal{W}_{stored}$  in the presence of the metal particle is dominated by its electric share  $\mathcal{W}_{stored}^{(e)}$ , which is given by [34], [43], [44], [45]

 $\mathcal{W}^{(e)}$  .

$$= \frac{\varepsilon_0}{4} \left( 1 + \frac{\partial(\omega \chi)}{\partial \omega} \right) \int_V \|\mathbf{E}_h\|^2 d^3 \mathbf{r} + \frac{\varepsilon_0}{4} \int_V \|\mathbf{E}_h\|^2 d^3 \mathbf{r}$$
 (44)

where  $V_e$  is the external space. Using the following identity (see (35) in [20] and [24]):

$$\int_{V_e} \|\mathbf{E}_h\|^2 d^3 \mathbf{r} = \left(\chi_h^{\parallel} - 1\right) \int_{V} \|\mathbf{E}_h\|^2 d^3 \mathbf{r}$$
 (45)

in (44), we obtain

$$\mathcal{W}_{\text{stored}}^{(e)} = \frac{\varepsilon_0}{4} \left( \chi_h^{\parallel} + \frac{\partial (\omega \chi)}{\partial \omega} \right) \int_V \|\mathbf{E}_h\|^2 d^3 \mathbf{r}. \tag{46}$$

Then, we evaluate the norm of the electric field in V

$$\int_{V} \|\mathbf{E}_{h}\|^{2} d^{3}\mathbf{r} = \frac{1}{4\pi\varepsilon_{0}^{2}\chi_{h}^{\parallel}} \oint_{S} \sigma_{h}^{*}(\mathbf{r}) \oint_{S} \frac{\sigma_{h}(\mathbf{r}')}{|\mathbf{r} - \mathbf{r}'|} dS' dS \quad (47)$$

where we have used (43), the divergence theorem, and  $\mathbf{E}_h \cdot \hat{\mathbf{n}} = -\sigma_h/(\varepsilon_0 \chi_h^{\parallel})$  on S.

In conclusion, by combining (47) and (46), we obtain

$$\mathcal{W}_{\text{stored}}^{(e)} = \beta(\omega) \frac{1}{8\pi \,\varepsilon_0} \oint_{S} \sigma_h^*(\mathbf{r}) \oint_{S} \frac{\sigma_h(\mathbf{r}')}{|\mathbf{r} - \mathbf{r}'|} dS' \, dS \qquad (48)$$

where

$$\beta(\omega) = \frac{1}{2\chi_{L}^{\parallel}} \left( \chi_{h}^{\parallel} + \frac{\partial(\omega\chi)}{\partial\omega} \right). \tag{49}$$

For a Drude metal with vanishing losses [see (42)], we have  $((\partial(\omega\chi))/\partial\omega) = -\chi(\omega)$ . Moreover by (7), at the resonance we have  $\chi(\omega_h) \approx -\chi_h^{\parallel}$ , thus  $\beta(\omega_h) \approx 1$ . In conclusion, we obtain

$$\mathscr{W}_{\text{stored}}^{(e)} = \frac{1}{8\pi\varepsilon_0} \oint_{S} \sigma_h^*(\mathbf{r}) \oint_{S} \frac{\sigma_h(\mathbf{r}')}{|\mathbf{r} - \mathbf{r}'|} dS' dS. \tag{50}$$

b) Radiated power: The power  $\mathscr{P}_h$  radiated in free space by the quasi-electrostatic current mode  $\mathbf{j}_h^{\parallel}$  with nonzero electric dipole moment is

$$\mathcal{P}_{h} = \frac{\mu_{0}\omega^{4}}{12\pi c} \|\mathbf{P}_{h}\|^{2} = \frac{\omega_{h}}{2} \frac{(k_{0}\ell_{c})^{3}}{6\pi \varepsilon_{0}} \frac{1}{\ell_{c}^{3}} \|\mathbf{P}_{h}\|^{2}$$

$$= \frac{\omega_{h}}{3} \frac{(k_{0}\ell_{c})^{3}}{\ell_{c}^{3}} \frac{1}{8\pi \varepsilon_{0}} \oint_{S} \sigma_{h}^{*}(\mathbf{r}) \oint_{S} \sigma_{h}(\mathbf{r}') |\mathbf{r} - \mathbf{r}'|^{2} d^{2}\mathbf{r} d^{2}\mathbf{r}'$$
(51)

where we used the identity  $\|\mathbf{P}_h\|^2 = -(1/2)\oint_S \sigma_h^*(\mathbf{r})\oint_S \sigma_h(\mathbf{r}')|\mathbf{r} - \mathbf{r}'|^2 d^3\mathbf{r}' d^3\mathbf{r}.$ 

c) Q factor: We now compute the Q factor using definition (41), assuming negligible dissipation losses in the material. By combining (50) and (51), we get (9). By exploiting the following identities:

$$\frac{1}{8\pi\varepsilon_{0}} \oint_{S} \sigma_{h}^{*}(\mathbf{r}) \oint_{S} \frac{\sigma_{h}(\mathbf{r}')}{|\mathbf{r} - \mathbf{r}'|} d^{2}\mathbf{r} d^{2}\mathbf{r}' = \frac{\omega^{2}}{2\varepsilon_{0}} \frac{\|\mathbf{j}_{h}^{\parallel}\|^{2}}{\chi_{h}^{\parallel}},$$

$$-\frac{1}{2} \int_{V} \sigma_{h}^{*}(\mathbf{r}) \int_{V} \sigma_{h}(\mathbf{r}') |\mathbf{r} - \mathbf{r}'|^{2} d^{3}\mathbf{r}' d^{3}\mathbf{r}$$

$$= \omega^{2} \left\| \int_{V} \mathbf{j}_{h}(\mathbf{r}) d^{3}\mathbf{r} \right\|^{2}. \tag{52}$$

Equation (9) becomes (10). It is worth noting that the expression (9) coincides with the one obtained by Vandenbosch [12] for an electrically small nondispersive tuned PEC radiator of the electric type.

2) High-Permittivity Dielectric Resonator: We now evaluate the stored energy, the radiated power, and the Q factor of a high-permittivity dielectric resonator with nondispersive susceptibility  $\chi(\omega) = \chi_0 \gg 1$  in the frequency range of interest.

a) Mean value of the stored energy: The stored energy  $\mathcal{W}_{\text{stored}}$  is the sum of the stored electric and magnetic energies. Starting from (44), the stored electric energy  $\mathcal{W}_{\text{stored}}^{(e)}$  can be rewritten as

$$\mathcal{W}_{\text{stored}}^{(e)} = \frac{\varepsilon_0}{4} \left( 1 + \frac{\partial \omega \chi_0}{\partial \omega} \right) \int_V \|\mathbf{E}_h\|^2 d^3 \mathbf{r} + \frac{\varepsilon_0}{4} \int_V \|\mathbf{E}_h\|^2 d^3 \mathbf{r} \approx \frac{\mu_0 \ell_c^2}{4\chi_h^2} \|\mathbf{j}_h\|^2$$
(53)

where we have exploited the fact that the second term dominates over the remaining two for  $\chi_0 \uparrow \infty$ , and the identity

$$\int_{V} \|\mathbf{E}_{h}\|^{2} d^{3}\mathbf{r} = \ell_{c}^{2} \mu_{0} \frac{\|\mathbf{j}_{h}\|^{2}}{\chi_{h}^{\perp} \varepsilon_{0} \chi_{0}}.$$
 (54)

The magnetic stored energy is given by

$$\mathcal{W}_{\text{stored}}^{(m)} = \frac{\mu_0}{4} \int_{V} \|\mathbf{H}_h\|^2 d^3 \mathbf{r} + \frac{\mu_0}{4} \int_{V_e} \|\mathbf{H}_h\|^2 d^3 \mathbf{r}$$
$$= \frac{1}{4\mu_0} \int_{V} \|\nabla \times \mathbf{A}_h\|^2 d^3 \mathbf{r} + \frac{1}{4\mu_0} \int_{V_e} \|\nabla \times \mathbf{A}_h\|^2 d^3 \mathbf{r}$$
(55)

where  $\mathbf{A}_h = \mu_0(\ell_c^2/\chi_h^\perp)\mathbf{j}_h^\perp$  is the vector potential associated with the magnetoquasistatic current mode. Using the identity

$$\nabla \times \mathbf{A} \cdot \nabla \times \mathbf{B} = \mathbf{A} \cdot \nabla \times \nabla \times \mathbf{B} + \nabla \cdot [\mathbf{A} \times \nabla \times \mathbf{B}] \quad (56)$$

and the property [28]  $\nabla \times \nabla \times \mathbf{A}_h = (\chi_h^{\perp}/\ell_c^2) \mathbf{A}_h$ ,  $\mathbf{r} \in V$ , we obtain

$$\mathcal{W}_{\text{stored}}^{(m)} = \frac{1}{4\mu_0} \int_V \mathbf{A}_h \cdot \nabla \times \nabla \times \mathbf{A}_h d^3 \mathbf{r} = \frac{\mu_0 \ell_c^2}{4\chi_h^{\perp}} \|\mathbf{j}_h^{\perp}\|^2. \quad (57)$$

Thus, the total stored energy  $W_{\text{stored}}$  is

$$\mathcal{W}_{\text{stored}} = \mathcal{W}_{\text{stored}}^{(e)} + \mathcal{W}_{\text{stored}}^{(m)} = \frac{\mu_0}{2} \frac{\ell_c^2}{\gamma_h^{\perp}} \|\mathbf{j}_h^{\perp}\|^2. \tag{58}$$

Using the following identity:

$$\frac{\mu_0}{2} \frac{\ell_c^2}{\mathbf{\gamma}_c^{\perp}} = \frac{1}{\|\mathbf{j}_L^{\perp}\|^2} \frac{\mu_0}{8\pi} \int_{V} \mathbf{j}_h^{\perp}(\mathbf{r}) \cdot \int_{V} \frac{\mathbf{j}_h^{\perp}(\mathbf{r}')}{|\mathbf{r} - \mathbf{r}'|} d^3 \mathbf{r}' d^3 \mathbf{r}$$
(59)

the expression of total stored energy is rewritten as

$$\mathcal{W}_{\text{stored}} = \mathcal{W}_{\text{stored}}^{(e)} + \mathcal{W}_{\text{stored}}^{(m)} = \frac{\mu_0}{2} \frac{\ell_c^2}{\chi_h^{\perp}} \|\mathbf{j}_h^{\perp}\|^2$$
$$= \frac{\mu_0}{8\pi} \int_V \mathbf{j}_h^{\perp}(\mathbf{r}) \cdot \int_V \frac{\mathbf{j}_h^{\perp}(\mathbf{r}')}{|\mathbf{r} - \mathbf{r}'|} d^3 \mathbf{r}' d^3 \mathbf{r}. \tag{60}$$

b) Radiated Power: The power  $\mathscr{P}_m$  radiated by the polarization current mode  $\mathbf{j}_h^{\perp}$  with nonvanishing magnetic dipole moment is given by

$$\mathcal{P}_{m} = \frac{\omega_{h}^{4}/c_{0}^{3}}{12c_{0}\pi} \|\mathbf{M}_{h}\|^{2} = \omega_{h} \frac{\mu_{0}}{12\pi} \left(\frac{\omega_{h}}{c_{0}}\ell_{c}\right)^{3} \frac{1}{\ell_{c}^{3}} \|\mathbf{M}_{h}\|^{2}$$

$$= \omega_{h} \frac{\mu_{0}}{48\pi} (k_{0}\ell_{c})^{3} \frac{1}{\ell_{c}^{3}} \int_{V} \mathbf{j}_{h}^{\perp}(\mathbf{r}) \cdot \int_{V} \mathbf{j}_{h}^{\perp}(\mathbf{r}') |\mathbf{r} - \mathbf{r}'|^{2} d^{3}\mathbf{r} d^{3}\mathbf{r}'.$$
(61)

c) Q factor: We now compute the Q factor using the definition. We assume that the material losses are negligible; thus, all the contribution to the power loss comes from the power radiated to infinity  $\mathcal{P}_m$ . By combining (60) and (61) and the definition (41), we obtain (21). It is worth noting that the expression (21) coincides with the one derived by Vandenbosch [12] for an electrically small tuned PEC radiator of the magnetic type.

# B. Resonant Modes of Surface Scatterers

1) Quasi-Electrostatic Resonances: Resonant electromagnetic scattering from a small-size non-magnetic scatterer occupying the surface S may occur when the imaginary part of its surface conductivity  $\Sigma$  is negative [38]. The corresponding quasi-electrostatic surface current modes are solution of the eigenvalue problem

$$\mathbf{j}_{h}^{\parallel}(\mathbf{r}) = \chi_{h}^{\parallel} \ell_{c} \, \hat{\mathbf{n}} \times \hat{\mathbf{n}} \times \nabla_{S} \oint_{S} \frac{\nabla_{S'} \cdot \mathbf{j}_{h}^{\parallel}(\mathbf{r}')}{4\pi \, |\mathbf{r} - \mathbf{r}'|} d^{2}\mathbf{r}' \quad \forall \mathbf{r} \in S \quad (62)$$

where  $\nabla_S$  is the surface gradient and  $\nabla_S'$  is the surface divergence. All the considerations made for the 3-D scatterers can be transplanted in this case, considering the scalar product  $\langle \mathbf{f}, \mathbf{g} \rangle_S = \int_S \mathbf{f}^* \cdot \mathbf{g} \, d^2 \mathbf{r}$ . The surface current density field  $\mathbf{J}^s(\mathbf{r})$  induced on the scatterer by an incident electric field  $\mathbf{E}_{inc}$  is given by [38]

$$\mathbf{J}^{s}(\mathbf{r}) \approx \sum_{h} \frac{\Sigma(\omega)\xi}{\xi + \chi_{h}^{\parallel} \Sigma(\omega)} \langle \mathbf{j}_{h}^{\parallel}, \mathbf{E}_{inc} \rangle_{S} \, \mathbf{j}_{h}^{\parallel}(\mathbf{r})$$
(63)

where  $\Sigma$  is the surface conductivity of the scatterer. The resonance frequency  $\omega_h$  of the hth quasi-electrostatic current mode is the frequency at which the real part of the denominator in the above equation vanishes [38]

$$\operatorname{Im}\{\Sigma(\omega_h)\} = -\frac{1}{\chi_h^{\parallel}} \left(\frac{\omega_h}{c_0} \ell_c\right). \tag{64}$$

The electric dipole moment  $\mathbf{P}_h$  of the surface current mode  $\mathbf{j}_h^{\parallel}$  is obtained by (4), where the integration is now performed on the surface, while the Q factor is still given by (10).

2) Quasi-Magnetostatic Resonances: Resonant electromagnetic scattering from a small-size non-magnetic scatterer occupying the surface S may occur when the imaginary part of its the surface conductivity  $\Sigma$  is positive and sufficiently high [38]. The corresponding quasi-magnetostatic resonances are associated with the eigenvalues of the integral operator that relates the vector potential to the surface current density

$$\mathbf{j}_{h}^{\perp}(\mathbf{r}) = -\frac{\chi_{h}^{\perp}}{\ell_{c}}\,\hat{\mathbf{n}}\times\hat{\mathbf{n}}\times\int_{S}\frac{\mathbf{j}_{h}^{\perp}(\mathbf{r}')}{4\pi\,|\mathbf{r}-\mathbf{r}'|}d^{2}\mathbf{r}'.$$
 (65)

All the considerations made for 3-D scatterers can then be transplanted to this scenario. If a surface with surface conductivity  $\Sigma$  is excited by an incident electric field  $\mathbf{E}_{inc}$ , the surface current density field  $\mathbf{J}^s(\mathbf{r})$  induced on the surface is given by [38]

$$\mathbf{J}^{s}(\mathbf{r}) \approx \sum_{h} \left( \frac{\Sigma(\omega)}{-1 + \xi \chi_{h}^{\perp}(\xi) \Sigma(\omega)} \right) \langle \mathbf{j}_{h}^{\perp}, \mathbf{E}_{inc} \rangle_{S} \, \mathbf{j}_{h}^{\perp}(\mathbf{r}). \quad (66)$$

The quasi-magnetostatic resonance frequency  $\omega_h$  of the *h*th mode is the frequency at which [38]

$$\operatorname{Im}\{\Sigma(\omega_h)\} = \frac{1}{\chi_h^{\perp}} \frac{c_0}{\omega_h \ell_c}.$$
 (67)

The corresponding size parameter at the resonance is given by (8). The magnetic dipole moment  $\mathbf{M}_h$  of the quasi-magnetostatic current mode  $\mathbf{j}_h^{\perp}$  is obtained by (17), where the integration is now performed on the surface  $\Sigma$ , while the Q factor is given by (21).

#### REFERENCES

- L. J. Chu, "Physical limitations of omni-directional antennas," J. Appl. Phys., vol. 19, no. 12, pp. 1163–1175, 1948.
- [2] H. A. Wheeler, "Fundamental limitations of small antennas," *Proc. IRE*, vol. 35, pp. 1479–1484, Dec. 1947.
- [3] R. F. Harrington, "Effect of antenna size on gain, bandwidth, and efficiency," J. Res. Nat. Bur. Standards, D, Radio Propag., vol. 64D, no. 1, p. 1, Jan. 1960.
- [4] R. E. Collin and S. Rothschild, "Evaluation of antenna Q," *IEEE Trans. Antennas Propag.*, vol. AP-12, no. 1, pp. 23–27, Jan. 1964.
- [5] J. S. McLean, "A re-examination of the fundamental limits on the radiation Q of electrically small antennas," *IEEE Trans. Antennas Propag.*, vol. 44, no. 5, p. 672, May 1996.
- [6] H. L. Thal Jr., "New radiation Q limits for spherical wire antennas," *IEEE Trans. Antennas Propag.*, vol. 54, no. 10, pp. 2757–2763, Oct. 2006.
- [7] M. Gustafsson, C. Sohl, and G. Kristensson, "Physical limitations on antennas of arbitrary shape," *Proc. Roy. Soc. A, Math., Phys. Eng. Sci.*, vol. 463, pp. 2589–2607, Jul. 2007.
- [8] M. Gustafsson, M. Cismasu, and B. L. G. Jonsson, "Physical bounds and optimal currents on antennas," *IEEE Trans. Antennas Propag.*, vol. 60, no. 6, pp. 2672–2681, Jun. 2012.
- [9] M. Gustafsson, D. Tayli, and M. Cismasu, "Physical bounds of antennas," Dept. Elect. Inf. Technol., Lund Univ., Lund, Sweden, Tech. Rep. LUTEDX TEAT-7240, 2015, pp. 1–38.
- [10] B. L. G. Jonsson and M. Gustafsson, "Stored energies in electric and magnetic current densities for small antennas," *Proc. Roy. Soc. A, Math.*, *Phys. Eng. Sci.*, vol. 471, no. 2176, 2015, Art. no. 20140897.
- [11] G. A. E. Vandenbosch, "Reactive energies, impedance, and Q factor of radiating structures," *IEEE Trans. Antennas Propag.*, vol. 58, no. 4, pp. 1112–1127, Apr. 2010.
- [12] G. A. E. Vandenbosch, "Simple procedure to derive lower bounds for radiation Q of electrically small devices of arbitrary topology," *IEEE Trans. Antenna Propag.*, vol. 59, no. 6, pp. 2217–2225, Jun. 2011.
- Trans. Antenna Propag., vol. 59, no. 6, pp. 2217–2225, Jun. 2011.
  [13] W. Geyi, P. Jarmuszewski, and Y. Qi, "The Foster reactance theorem for antennas and radiation Q," *IEEE Trans. Antennas Propag.*, vol. 48, no. 3, pp. 401–408, Mar. 2000.
- [14] W. Geyi, "A method for the evaluation of small antenna Q," *IEEE Trans. Antennas Propag.*, vol. 51, no. 8, pp. 2124–2129, Aug. 2003.
- [15] J. Chalas, K. Sertel, and J. L. Volakis, "Computation of the Q limits for arbitrary-shaped antennas using characteristic modes," *IEEE Trans. Antennas Propag.*, vol. 64, no. 7, pp. 2637–2647, Jul. 2016.
- [16] M. Capek and L. Jelinek, "Optimal composition of modal currents for minimal quality factor Q," *IEEE Trans. Antennas Propag.*, vol. 64, no. 12, pp. 5230–5242, Dec. 2016.
- [17] L. Jelinek and M. Capek, "Optimal currents on arbitrarily shaped surfaces," *IEEE Trans. Antennas Propag.*, vol. 65, no. 1, pp. 329–341, Jan. 2017.
- [18] M. Capek, M. Gustafsson, and K. Schab, "Minimization of antenna quality factor," *IEEE Trans. Antennas Propag.*, vol. 65, no. 8, pp. 4115–4123, Aug. 2017.
- [19] M. Capek, L. Jelinek, and M. Masek, "A role of symmetries in evaluation of fundamental bounds," *IEEE Trans. Antennas Propag.*, vol. 69, no. 11, pp. 7729–7742, Nov. 2021.
- [20] A. D. Yaghjian, "Overcoming the chu lower bound on antenna Q with highly dispersive lossy material," *IET Microw., Antennas Propag.*, vol. 12, no. 4, pp. 459–466, Mar. 2018.
- [21] S. A. Maier, Plasmonics: Fundamentals and Applications. New York, NY, USA: Springer, 2007.
- [22] L. Novotny and B. Hecht, *Principles of Nano-Optics*. Cambridge, U.K.: Cambridge Univ. Press, 2006.

- [23] D. R. Fredkin and I. D. Mayergoyz, "Resonant behavior of dielectric objects (electrostatic resonances)," *Phys. Rev. Lett.*, vol. 91, no. 25, 2003, Art. no. 253902.
- [24] I. Mayergoyz, D. Fredkin, and Z. Zhang, "Electrostatic (plasmon) resonances in nanoparticles," *Phys. Rev. B, Condens. Matter*, vol. 72, no. 15, 2005, Art. no. 155412.
- [25] D. C. Tzarouchis, P. Yla-Oijala, and A. Sihvola, "Resonant scattering characteristics of homogeneous dielectric sphere," *IEEE Trans. Antennas Propag.*, vol. 65, no. 6, pp. 3184–3191, Jun. 2017.
- [26] D. Tzarouchis and A. Sihvola, "Light scattering by a dielectric sphere: Perspectives on the mie resonances," *Appl. Sci.*, vol. 8, no. 2, p. 184, Jan. 2018.
- [27] K. Koshelev and Y. Kivshar, "Dielectric resonant metaphotonics," ACS Photon., vol. 8, no. 1, pp. 102–112, Jan. 2021.
- [28] C. Forestiere et al., "Magnetoquasistatic resonances of small dielectric objects," *Phys. Rev. Res.*, vol. 2, Feb. 2020, Art. no. 013158.
- [29] C. Forestiere and G. Miano, "Time-domain formulation of electromagnetic scattering based on a polarization-mode expansion and the principle of least action," *Phys. Rev. A, Gen. Phys.*, vol. 104, no. 1, Jul. 2021, Art. no. 013512.
- [30] R. J. Garbacz, "Modal expansions for resonance scattering phenomena," Proc. IEEE, vol. 53, no. 8, pp. 856–864, Aug. 1965.
- [31] C. Forestiere, G. Miano, and G. Rubinacci, "Resonance frequency and radiative Q-factor of plasmonic and dielectric modes of small objects," *Phys. Rev. Res.*, vol. 2, Nov. 2020, Art. no. 043176.
- [32] D. E. Gómez, Z. Q. Teo, M. Altissimo, T. J. Davis, S. Earl, and A. Roberts, "The dark side of plasmonics," *Nano Lett.*, vol. 13, no. 8, pp. 3722–3728, Aug. 2013.
- [33] B. L. G. Jonsson and M. Gustafsson, "Stored energies for electric and magnetic current densities," 2016, arXiv:1604.08572.
- [34] J. D. Jackson, Classical Electrodynamics. Maryland, MD, USA: American Association of Physics Teachers, 1999.
- [35] A. D. Yaghjian, "Force and hidden momentum for classical microscopic dipoles," *Prog. Electromagn. Res. B*, vol. 82, pp. 165–188, 2018.
- [36] A. Yaghjian, M. Gustafsson, and A. L. Jonsson, "Minimum Q for lossy and lossless electrically small dipole antennas," *Prog. Electromagn. Res.*, vol. 143, pp. 641–673, 2013.
- [37] I. D. Mayergoyz, Z. Zhang, and G. Miano, "Analysis of dynamics of excitation and dephasing of plasmon resonance modes in nanoparticles," *Phys. Rev. Lett.*, vol. 98, no. 14, Apr. 2007, Art. no. 147401.
- [38] C. Forestiere, G. Gravina, G. Miano, M. Pascale, and R. Tricarico, "Electromagnetic modes and resonances of two-dimensional bodies," *Phys. Rev. B, Condens. Matter*, vol. 99, no. 15, Apr. 2019, Art. no. 155423.
- [39] M. Pascale, G. Miano, R. Tricarico, and C. Forestiere, "Full-wave electromagnetic modes and hybridization in nanoparticle dimers," *Sci. Rep.*, vol. 9, no. 1, p. 14524, Oct. 2019.
- [40] M. Pascale, S. A. Mann, C. Forestiere, and A. Alù, "Bandwidth of singular plasmonic resonators in relation to the chu limit," ACS Photon., vol. 8, no. 11, pp. 3249–3260, Nov. 2021.
- [41] IEEE Standard for Definitions of Terms for Antennas, IEEE Standard 145-2013 (Revision IEEE Standard 145-1993), Mar. 2014, pp. 1–50.
- [42] K. Schab et al., "Energy stored by radiating systems," *IEEE Access*, vol. 6, pp. 10553–10568, 2018.
- [43] L. Brillouin, Wave Propagation and Group Velocity. New York, NY, USA: Academic, Oct. 2013.
- [44] L. D. Landau, J. S. Bell, M. J. Kearsley, L. P. Pitaevskii, E. M. Lifshitz, and J. B. Sykes, *Electrodynamics of Continuous Media*. Amsterdam, The Netherlands: Elsevier, Oct. 2013.
- [45] A. D. Yaghjian and S. R. Best, "Impedance, bandwidth, and Q of antennas," *IEEE Trans. Antennas Propag.*, vol. 53, no. 4, pp. 1298–1324, Apr. 2005.



**Mariano Pascale** received the B.Sc., M.Sc., and Ph.D. degrees in electronic engineering from the Università degli Studi di Napoli Federico II, Naples, Italy, in 2014, 2016, and 2021, respectively.

In 2017, he was a Cooperative Associate with the BEams Department, Accelerators and Beam Physics Group, Hadron Synchrotron Collective Effects Section (BE-ABP-HSC), European Organization for Nuclear Research (CERN), Geneva, Switzerland. From 2019 to 2020, he was a Visiting Research Scholar with the Photonics Initiative,

Advanced Science Research Center, City University of New York (CUNY),

New York, NY, USA. Since 2021, he has been a Post-Doctoral Researcher with the Thermal Photonics Group, Institut de Ciencies Fotoniques (ICFO), Barcelona, Spain. His research interests include radiative heat transfer, nanophotonics, electromagnetic scattering, and computational electromagnetism.



**Sander A. Mann** received the B.Sc. degree in physics and the M.Sc. degree in energy science from Utrecht University, Utrecht, The Netherlands, in 2010 and 2012, respectively, and the Ph.D. degree from AMOLF, Amsterdam, The Netherlands, and the University of Amsterdam, Amsterdam, in 2016.

After obtaining his Ph.D. degree, he became a Post-Doctoral Fellow at The University of Texas at Austin, Austin, TX, USA. He is currently a Post-Doctoral Fellow with the Advanced Science Research Center (ASRC), City University of New

York (CUNY), New York, NY, USA.

Dr. Mann has received the two-year Rubicon Fellowship from the Dutch Research Council (NWO).



**Dimitrios C. Tzarouchis** (Member, IEEE) received the Diploma, the B.Sc. and M.Sc. degrees in electrical and computer engineering from the Aristotle University of Thessaloniki, Thessaloniki, Greece, in 2013, and the Ph.D. degree from Aalto University, Espoo, Finland, in 2019.

Following his post-doctoral appointment at the University of Pennsylvania, Philadelphia, PA, USA, he currently serves as a Senior Metamaterials Engineer at Meta Materials Inc., Athens, Greece, where he drives the research and development of

cutting-edge metamaterial technologies. He is an expert in theoretical and applied electromagnetics and circuits. He has made numerous significant contributions to the field through his published works in journals and conference proceedings, covering a broad range of topics, such as electromagnetic scattering theory, plasmonics, antenna theory, numerical methods, modeling, metamaterials/metasurfaces, and analog computing with electromagnetic waves

Dr. Tzarouchis has served as the Secretary for the IEEE AP/MTT/ED Finnish Chapter from 2017 to 2019. His achievements in the field have earned him several awards and honors, including the 2015 IEEE Antennas and Propagation Society Doctoral Research Grant, the 2017 Nokia Scholarship Grant, the 2018 IEEE Photonics Graduate Fellowship, multiple Young Scientist Awards (URSI-GASS 2017, URSI AT-RASC 2018, URSI EMTS 2019, URSI GASS 2020), the Best Student Paper Award (Second Prize) at PIERS 2017 and URSI-AT-RASC 2018, and the 2021 Optica Innovation Technical Group Prize. He received the Best Thesis Award during his Ph.D. degree in 2020. He currently holds the position of the Chair (2021–2023) for the Photonic Metamaterial Technical Group of Optica (formerly OSA) and serves as an Early Career Representative (2020–2026) for Commission B (Fields and Waves).



**Giovanni Miano** received the Laurea (summa cum laude) and Ph.D. degrees in electrical engineering from the University of Naples Federico II, Naples, Italy, in 1983 and 1989, respectively.

From 1984 to 1985, he was with the PS Division, European Organization for Nuclear Research (CERN), Geneva, Switzerland. Since 1989, he has been a Full Professor with the Faculty of Engineering, University of Naples Federico II. From 2005 to 2009, he was the Director of the Dipartimento di Ingegneria Elettrica. In 1996, he was

the Visiting Scientist of the GSI Laboratories, Darmstadt, Germany. In 1999, he was a Visiting Professor with the Department of Electrical Engineering, University of Maryland, College Park, MD, USA. He is the author or a coauthor of more than 100 articles published in international journals, 100 papers published in international conference proceedings, two items in the Wiley Encyclopedia of Electrical and Electronic Engineering (New York: Wiley, 1999), and the monograph Transmission Lines and Lumped Circuits (New York: Academic, 2001). His current research interests include ferromagnetic materials, nonlinear dielectrics, plasmas, electrodynamics of continuum media, nanotechnology, and modeling of lumped and distributed circuits.



**Andrea Alù** (Fellow, IEEE) received the Laurea, M.S., and Ph.D. degrees from the University of Roma Tre, Rome, Italy, in 2001, 2003, and 2007, respectively.

He is currently a Distinguished Professor with the City University of New York (CUNY), New York, NY, USA; the Founding Director of the Photonics Initiative, Advanced Science Research Center, CUNY; the Einstein Professor of physics with the Graduate Center, CUNY; a Professor of electrical engineering with the City College of New York,

New York; and the Senior Research Scientist and an Adjunct Professor with the The University of Texas at Austin, Austin, TX, USA. After performing post-doctoral research at the University of Pennsylvania, Philadelphia, PA, USA, in 2009, he joined the faculty of The University of Texas at Austin, where he was the Temple Foundation Endowed Professor until 2018. In 2015, he was the Royal Netherlands Academy of Arts and Sciences (KNAW) Visiting Professor at the AMOLF Institute, Amsterdam, The Netherlands. His research interests cover metamaterials, applied electromagnetics, optics, nanophotonics, polaritonics, and acoustics.

Dr. Alù was a member of the Administrative Committee of the IEEE Antennas and Propagation Society and the IEEE joint AP-S and MTT-S Chapter Chair for Central Texas. He has been a Simons Investigator in physics since 2016 and a Full Member of URSI. He is a fellow of NAI, AAAS, MRS, OSA, SPIE, and APS. He is also the President of the Metamorphose Virtual Institute for Artificial Electromagnetic Materials and Metamaterials and the Director of the Simons Collaboration on Extreme Wave Phenomena, Over the past few years, he has received several awards for his research activities, including the URSI Commission B in 2004, 2007, and 2010, the Young Scientist Awards from URSI General Assembly in 2005, the NSF CAREER Award in 2010, the AFOSR and the DTRA Young Investigator Awards in 2010 and 2011, the URSI Issac Koga Gold Medal in 2011, the SPIE Early Career Investigator Award in 2012, the OSA Adolph Lomb Medal in 2013, the IUPAP Young Scientist Prize in Optics in 2013, the Franco Strazzabosco Award for Young Engineers in 2013, the IEEE MTT Outstanding Young Engineer Award in 2014, the NSF Alan T. Waterman Award in 2015, the ICO Prize in Optics in 2016, the Inaugural MDPI Materials Young Investigator Award in 2016, the Kavli Foundation Early Career Lectureship in Materials Science in 2016, the Inaugural ACS Photonics Young Investigator Award Lectureship in 2016, the Edith and Peter O'Donnell Award in Engineering in 2016, the IUMRS Young Researcher Award in 2018, the DoD Vannevar Bush Faculty Fellowship in 2019, the IEEE Kiyo Tomiyasu Award in 2020, the Blavatnik National Award in Physical Sciences and Engineering in 2021, the AAAFM Heeger Award in 2021, and the Dan Maydan Prize in Nanoscience

in 2021. His students have also received several awards, including several Student Paper Awards at IEEE Antennas and Propagation and URSI Symposia. He has been serving on the Editorial Board for Reviews of Electromagnetics, Physical Review B, Advanced Optical Materials, Laser and Photonics Reviews, New Journal of Physics, EPJ Applied Metamaterials, and Metamaterials (ISTE). He has served as an Associate Editor for IEEE ANTENNAS AND WIRELESS PROPAGATION LETTERS, Optics Express, Applied Physics Letters, Materials (MDPI), Scientific Reports, Metamaterials, and Advanced Electromagnetics. He has guest edited special issues for the IEEE JOURNAL OF SELECTED TOPICS IN QUANTUM ELECTRONICS, PROCEEDINGS OF IEEE (twice), IEEE TRANSACTIONS ON ANTENNAS AND PROPAGATION, IEEE ANTENNAS AND WIRELESS PROPAGATION LETTERS (twice), Nanophotonics, Journal of Optics, Journal of the Optical Society of America A, Journal of the Optical Society of America B, Photonics and Nanostructures: Fundamentals and Applications, Optics Communications, Metamaterials, and Sensors on a variety of topics involving metamaterials, plasmonics, optics, and electromagnetic theory. He is the Editor-in-Chief of Optical Materials Express. He has been an OSA Traveling Lecturer since 2010 and an IEEE AP-S Distinguished Lecturer since 2014. He has been a Highly Cited Researcher (Clarivate Web of Science) since 2017.



Carlo Forestiere received the B.Sc., M.Sc. (summa cum laude), and Ph.D. degrees in electrical engineering from the University of Naples Federico II, Naples, Italy, in 2005, 2007, and 2010, respectively.

From 2011 to 2014, he was a Post-Doctoral Research Fellow with Boston University, Boston, MA, USA. He is currently an Associate Professor with the University of Naples Federico II. He has authored or coauthored more than 60 scientific contributions in peer-reviewed journal articles and book chapters and has given more than 20 invited talks

and seminars. His research interests include applied electromagnetism and quantum technologies and currently focus on nanophotonics, electromagnetic scattering, and computational electromagnetics.